Cordova, J.L., Mulcahy, S.R., Schermer, E.R., and Webb, L.E., 2018, Subduction initiation and early evolution of the Easton metamorphic suite, northwest Cascades, Washington: Lithosphere, https://doi.org/10.1130/L1009.1.

GSA DATA REPOSITORY ITEM 2018416

ADDITIONAL DATA REPOSITORY ITEMS

Table DR1

Table DR2

TABLE OF CONTENTS

DECRIPTION OF EPMA METHODS

The chemistry of amphibole, white mica, chlorite, and garnet was investigated to classify mineral species, determine compositional trends, and estimate metamorphic temperatures during crystallization. Mineral compositions were measured by electron probe microanalysis (EPMA) using a Cameca SX-50 at the University of British Columbia, Canada (Table DR1). A 15 kV accelerating voltage and a 20 nA beam current was used for all samples. A beam diameter of 10 microns was used for white mica and chlorite and 5 microns for amphibole and garnet. Natural and synthetic standards were used for calibration. Mineral formulas and ferric iron contents were calculated using the program AX (Powell and Holland, 1994). Amphiboles were classified following the scheme of Hawthorne (2012) and using the Excel spreadsheet of Locock (2014). Mineral compositions are plotted in Figure 6.

PRESSURE-TEMPERATURE PLOTS

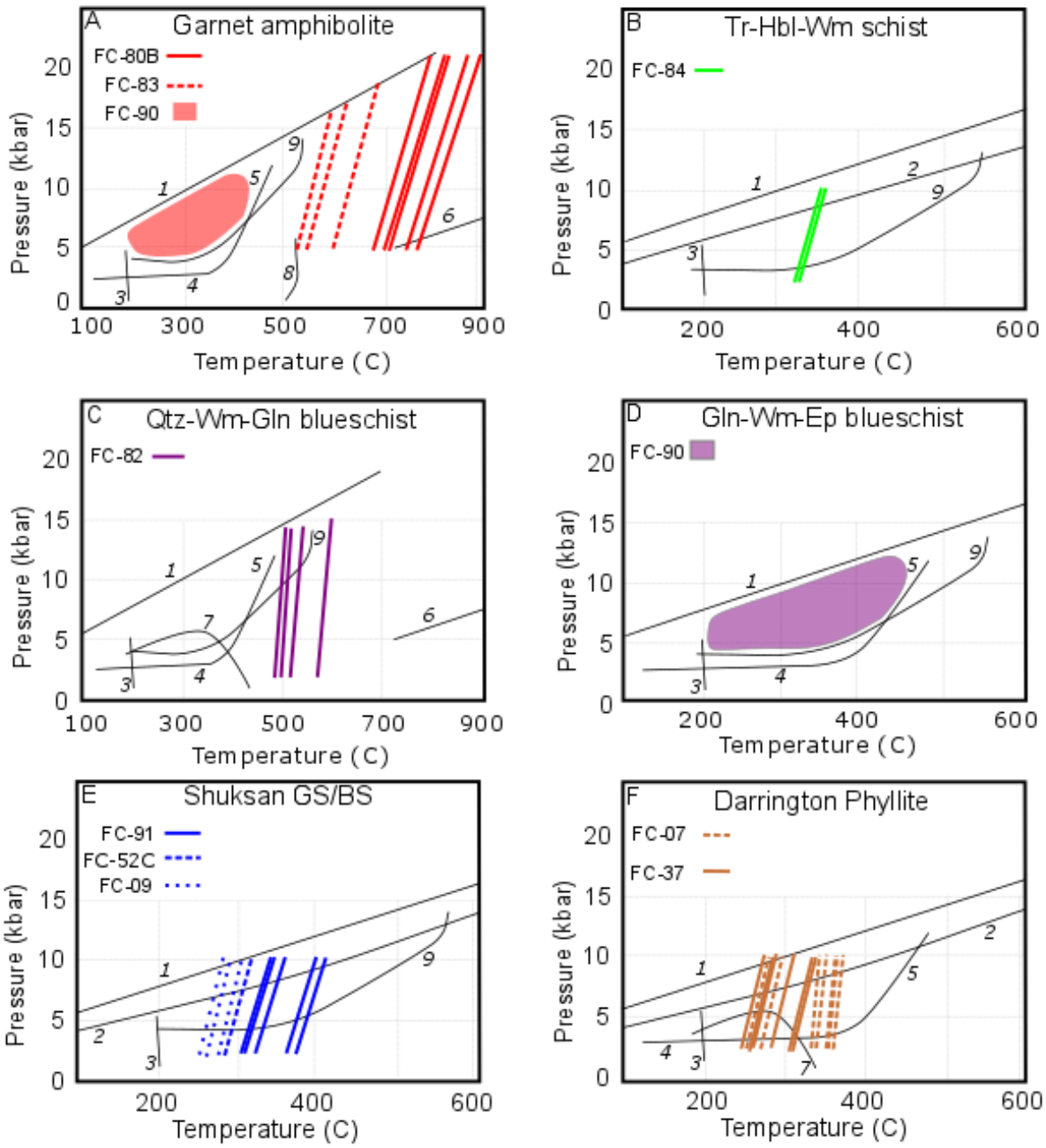

Figure DR1: PT diagrams for the Easton Metamorphic Suite are shown above by rock unit. Colored lines are the locations of Fe/Mg exchange reactions determined by Thermocalc for

garnet-hornblende pairs in A, mica-chlorite pairs in B, E, and F, and garnet-phengite pairs in C. For D the mineral assemblage was used to bracket pressure and temperature. The locations of metamorphic reactions are shown with black lines: 1) Ab=Jd+Q (Thermocalc), 2) Cal=Arag (Thermocalc), 3) Anl+Q=Ab+H2O (Liou, 1971), 4) Wa=Lws+Q (Liou, 1971), 5) Lws=An+Q+F (Crawford and Fyfe, 1965), 6) Grt in (Spear, 2014), 7) Prh= Lws+Grs+Qtz (Perkins, et al., 1979), 8) Act+Chl+E+Ab+Q=Hbl+Pl+Q+F (Apted and Liou, 1983), and 9) Ab+Mm=Gln (Maresch, 1977).

$^{40}Ar/^{39}Ar$ GEOCHRONOLOGY METHODS DESCRIPTION

$^{40}Ar/^{39}Ar$ analyses were performed at the University of Vermont Noble Gas Geochronology Laboratory. Inclusion-free mineral grains were handpicked from crushed rock samples under a bioptic microscope after having been washed, sonicated, and dried to remove any adhering particulate matter. Grains from each sample were loaded into aluminum foil packets, arranged in a suprasil vial, and placed in an aluminum canister for irradiation. Samples were irradiated with multigrain aliquots of Fish Canyon Tuff sanidine to act as a flux monitor (28.201 Ma; Kuiper et al., 2008) to monitor the neutron dose, and Ca and K salts were also irradiated to determine corrections for interfering nuclear reactions. Samples were irradiated for 14 hours at the Cadmium-Lined In-Core Irradiation Tube (CLICIT) reactor of Oregon State University, Corvallis, Oregon, USA.

Laser step heating for $^{40}Ar/^{39}Ar$ dating was conducted with a Santa Cruz Laser Microfurnace 75 W diode laser system. With the exception of flux monitors and muscovite, samples were loaded directly into wells in a copper sample holder. Sanidine and muscovite grains were loaded into degassed Nb foil packets before being loaded in the wells in the sample holder. The gas released during heating was purified with SAES getters and argon isotopes were analyzed on a Nu Instruments Noblesse magnetic sector noble gas mass spectrometer in peak-

hopping mode during step-heating analyses. Data from samples and flux monitors were corrected for blanks, mass discrimination, atmospheric argon, neutron-induced interfering isotopes, and the decay of ^{37}Ar and ^{39}Ar. Mass discrimination was calculated by analyzing known aliquots of atmospheric argon for which the measured $^{40}Ar/^{36}Ar$ was compared with an assumed atmospheric value of 298.56 (Lee et al., 2006). Correction factors used to account for interfering nuclear reactions for the irradiated samples are: $(^{40}Ar/^{39}Ar)_K = 5.4 \times 10^{-4} \pm 1.4 \times 10^{-4}$ (Jicha and Brown, 2014), $(^{36}Ar/^{37}Ar)_{Ca} = 2.65 \times 10^{-4} \pm 0.22 \times 10^{-4}$ (Renne et al., 2013), and $(^{39}Ar/^{37}Ar)_{Ca} = 6.95 \times 10^{-4} \pm 0.09 \times 10^{-4}$ (Renne et al., 2013). A linear interpolation was used to calculate J factors for samples based on sample position between flux monitor packets in the irradiation tube. All ages were calculated using the isotope decay constants recommended by Steiger and Jäger (1977). The age calculations for inverse isochron and apparent age data were achieved using both an in-house data reduction program and Isoplot 3.0 (Ludwig, 2003).

Weighted mean ages are reported, and plateau ages are reported if sufficient criteria were met (as noted in main text). Errors on plateaus and weighted mean ages are quoted at the 2σ level and include precision associated with measurement of the irradiation parameter, J, for flux monitors.

PHOTOMICROGRAPHS OF GEOCHRONOLOGY SAMPLES

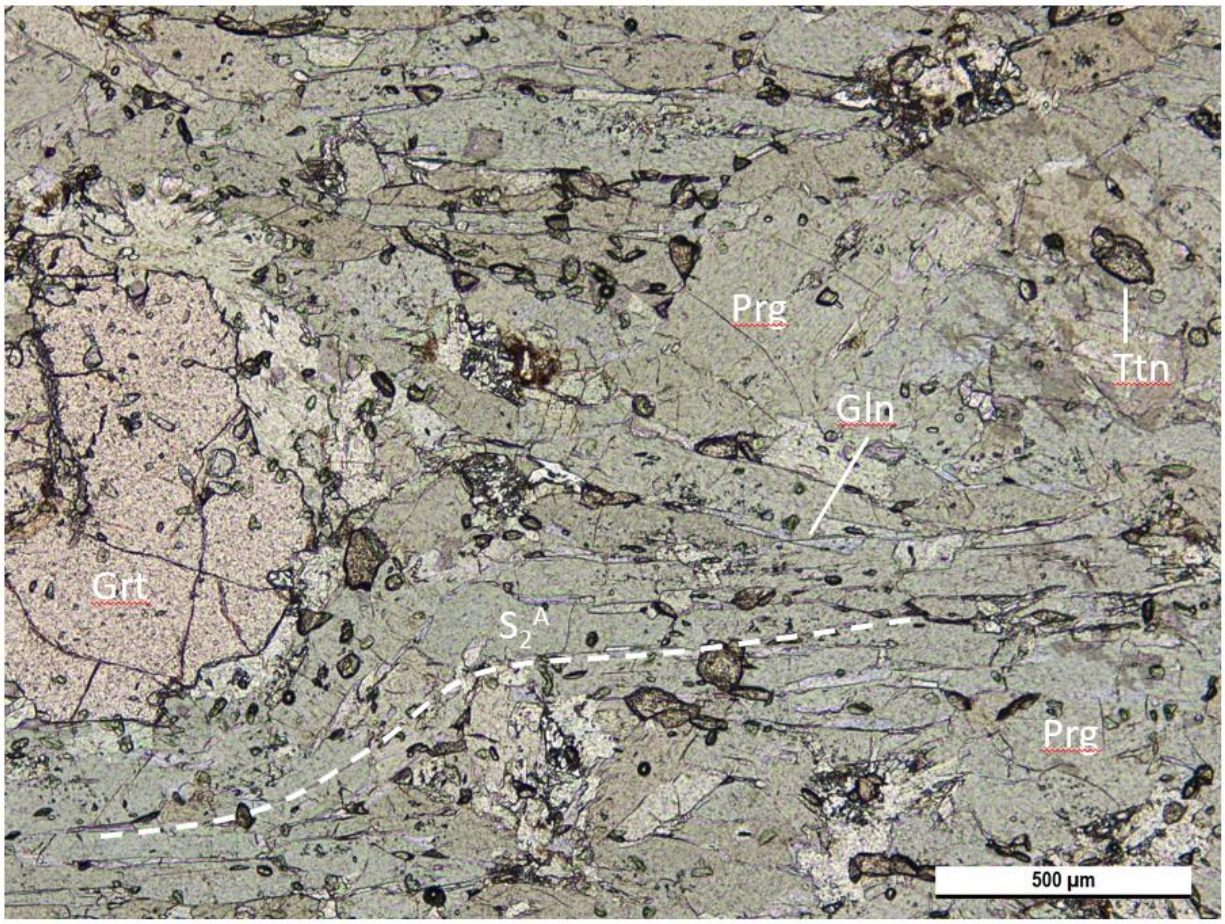

Figure DR2: Sample FC-83, showing a primary garnet-pargasite assemblage in the S_2^A fabric, with retrograde intergranular glaucophane.

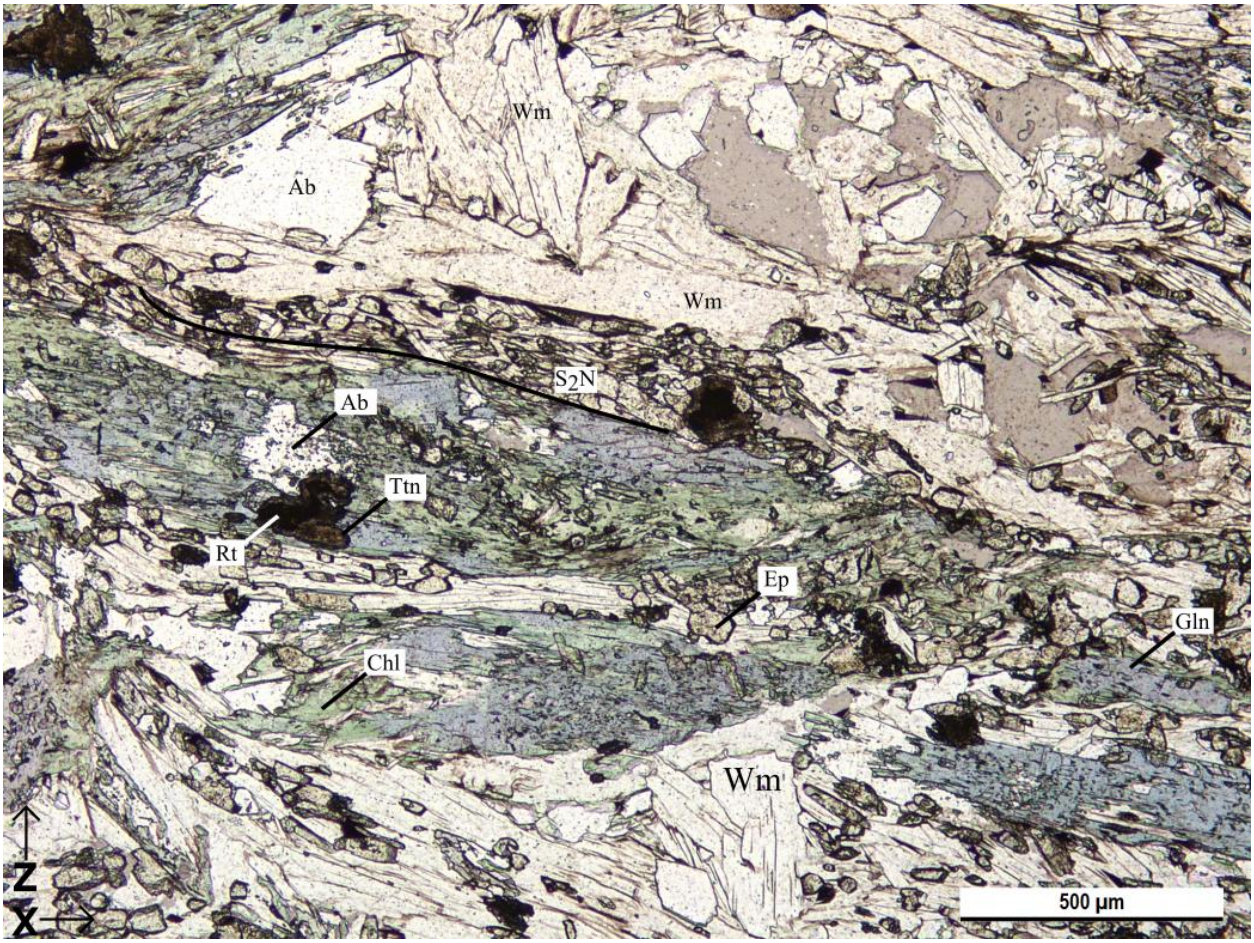

Figure DR3: Photomicrograph of geochronology sample FC-90, with coarse mineral phases in the S_2^N fabric labelled with text.

99

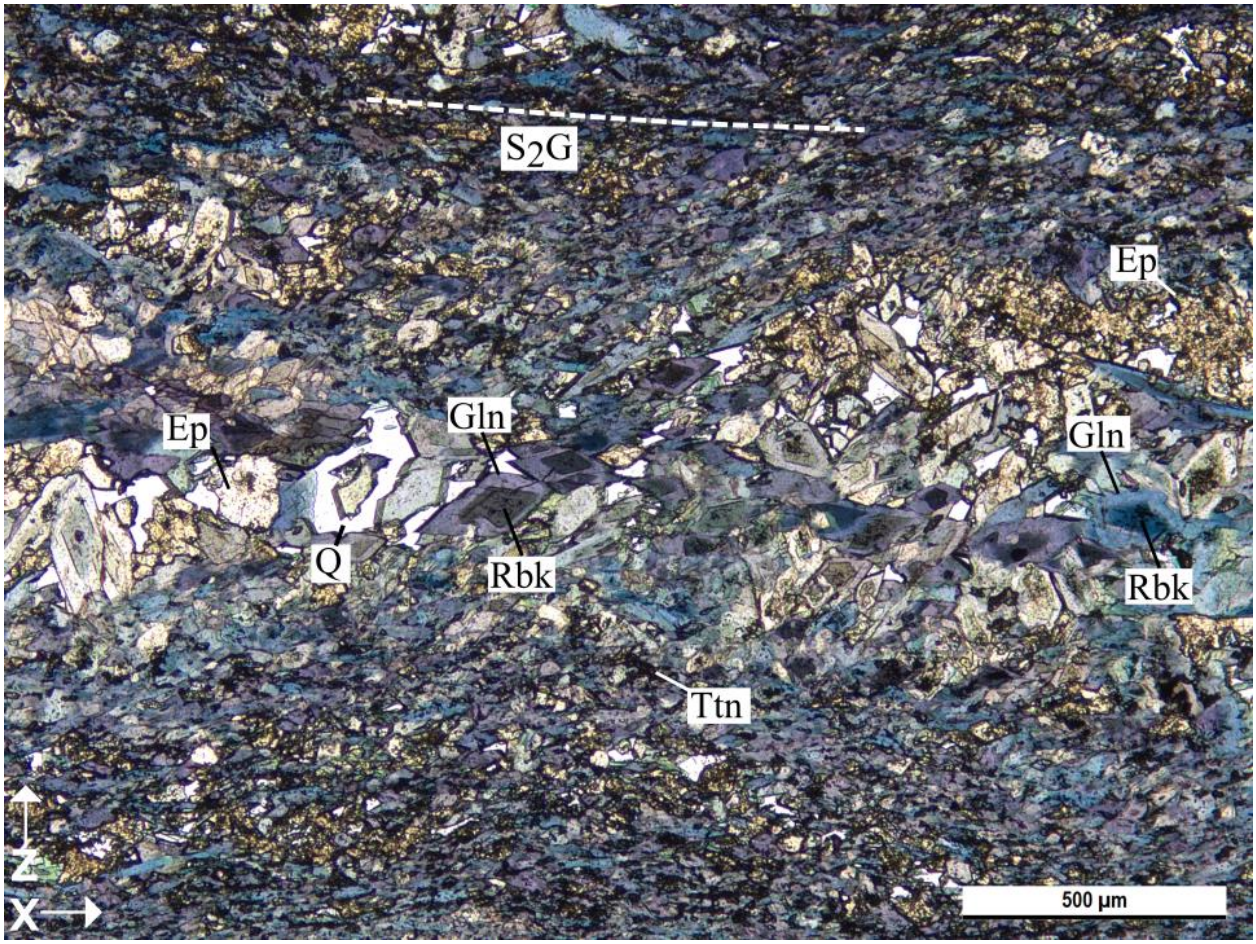

Figure DR4: Geochronology sample FC-36, showing sodic amphiboles with riebeckite cores and glaucophane rims, alongside other coarse mineral phases labelled with text.

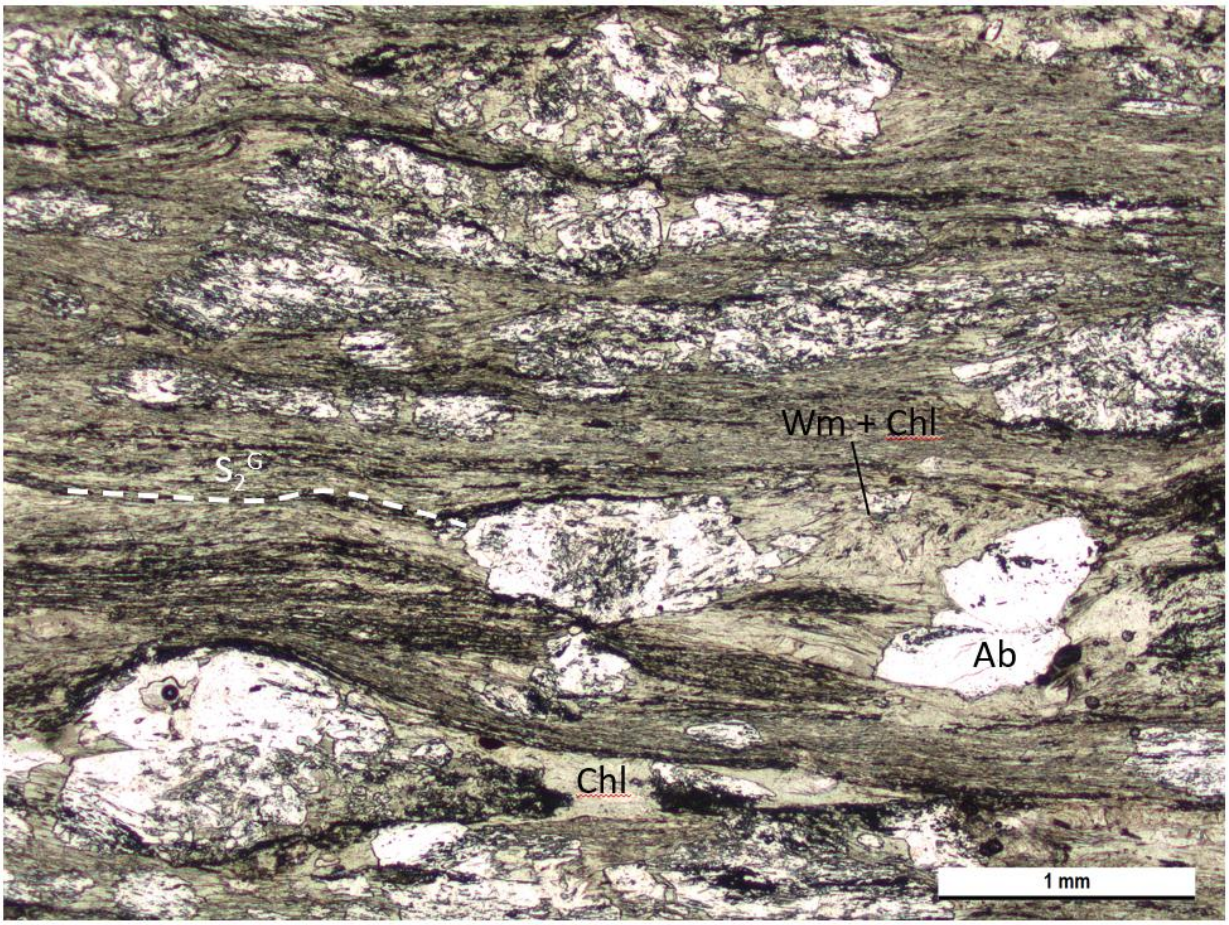

Figure DR5: Geochronology sample FC-52C showing phengite and chlorite in the S_2^G fabric, with albite.

107

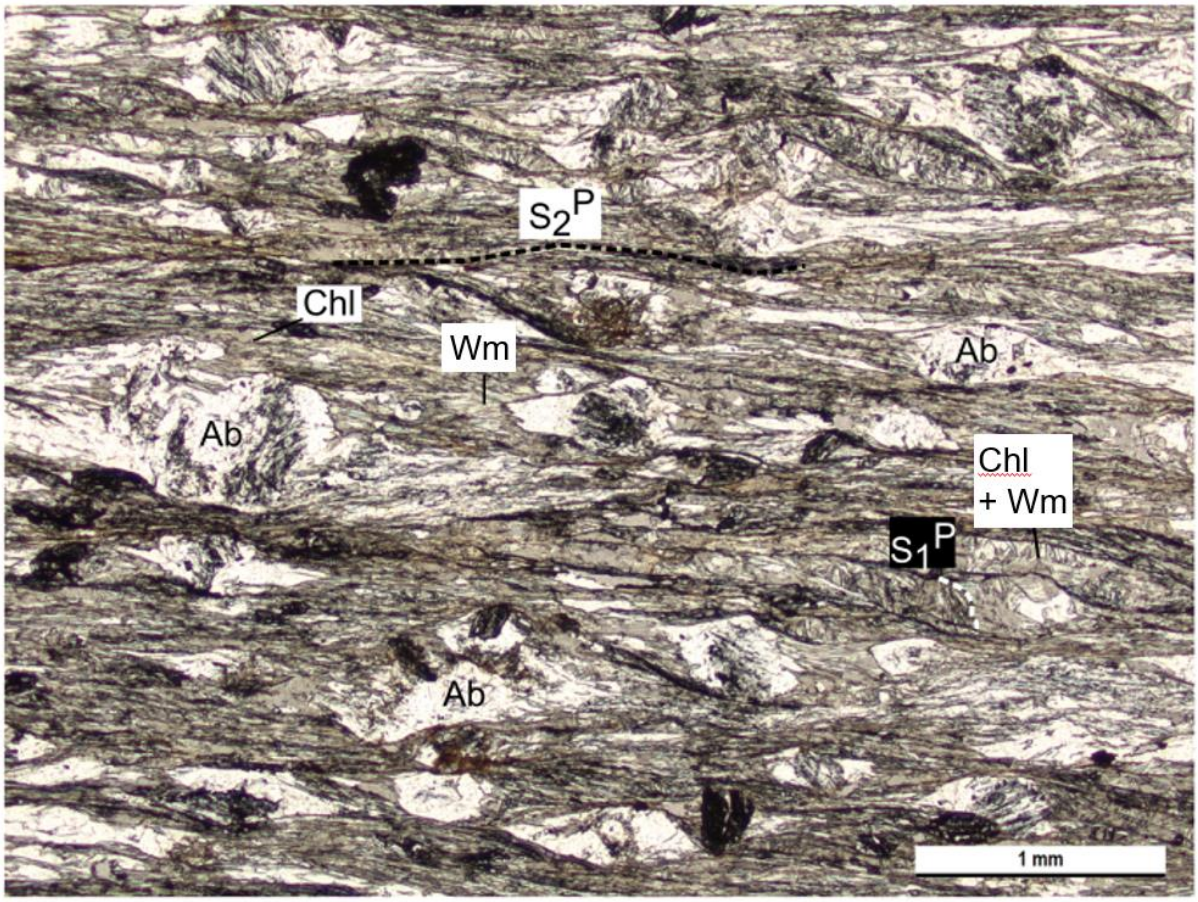

Figure DR6: Geochronology sample FC-37 showing white mica and chlorite in the S_2^P fabric cross-cutting S_1^P, with finer-grained white mica and chlorite.

108

REFERENCES CITED

Andersson, J.O., Helander, T., Hoglung, L., Shi, P.F., and Sundman, B., 2002, Thermocalc and DICTRA, Computational Tools for Computational Science. Calphad, 26, p. 273-312.

Apted, J., M., Liou, J., G., 1983, Phase relations among greenschist, epidote-amphibolite, and amphibolite in a basaltic system. American Journal of Science, volume 283-A, P. 328-354.

Crawford, W.A., and Fyfe, W.S., 1965, Lawsonite equilibria: American Journal of Science, v. 263, p. 262–270, doi: 10.2475/ajs.263.3.262.

Hawthorne, F.C., Oberti, R., Harlow, G.E., Maresch, W.V., Martin, R.F., Schumacher, J.C., and Welch, M.D., 2012, Nomenclature of the amphibole supergroup: American Mineralogist, v. 97, p. 2031–2048, doi: 10.2138/am.2012.4276.

Jicha, B.R. and Brown, F.H., 2014. An age for the Korath Range, Ethiopia and the viability of $^{40}Ar/^{39}Ar$ dating of kaersutite in Late Pleistocene volcanics. Quaternary Geochronology, 21, pp.53-57.

131 Kuiper, K. F., Deino, A., Hilgen, F. J., Krijgsman, W., Renne, P. R., & Wijbrans, A. J., 2008.
132 Synchronizing rock clocks of Earth history. science, 320(5875), 500-504.
133 Lee, J.-Y., Marti, K., Severinghaus, J.P., Kawamura, K., Yoo, H.-S., Lee, J.B. & Kim, J.S. 2006.
134 A redetermination of the isotopic abundances of atmospheric Ar. Geochimica et
135 Cosmochimica Acta, 70, 4507–4512, doi: http://dx.doi.org/10.1016/j.gca.2006.06.1563.
136 Liou, J.G., 1971, P—T Stabilities of Laumontite, Wairakite, Lawsonite, and Related Minerals in
137 the System CaAl2Si2O8-SiO2-H2O: Journal of Petrology, v. 12, p. 379–411, doi:
138 10.1093/petrology/12.2.379.
139 Locock, A.J., 2014, An Excel spreadsheet to classify chemical analyses of amphiboles following
140 the IMA 2012 recommendations: Computers & Geosciences, v. 62, p. 1–11, doi:
141 10.1016/j.cageo.2013.09.011.
142 Ludwig, K.R., 2003. Isoplot/EX, rev. 3.00, a Geochronological Toolkit for Microsoft Excel:
143 Berkeley Geochronology Center Special Publication, v. 4, 71 pp.
144 Maresch, W.., 1977, Experimental studies on glaucophane: An analysis of present knowledge:
145 Tectonophysics, v. 43, p. 109–125, doi: 10.1016/0040-1951(77)90008-7.
146 Perkins, D., Westrum, E.F., and Essene, E.J., 1980, The thermodynamic properties and phase
147 relations of some minerals in the system CaO-AI2O3-SiO2-H2O: Geochimica et
148 Cosmochimica Acta, v. 44, p. 61–84.
149 Powell, R., and Holland, T., 1994, Optimal geothermometry and geobarometry: American
150 Mineralogist, v. 79, p. 120–133.
151 Renne, P.R., Deino, A.L., Hilgen, F.J., Kuiper, K.F., Mark, D.F., Mitchell, W.S., Morgan, L.E.,
152 Mundil, R. and Smit, J., 2013. Time scales of critical events around the Cretaceous-
153 Paleogene boundary. Science, 339(6120), pp.684-687.

Spear, F.S., 1995, Metamorphic Phase Equilibria and Pressure-Temperature-time paths: Mineralogical Society of America, Washington D.C., p. 439

Steiger, R.H. & Jäger, E. 1977. Subcommission on geochronology: Convention on the use of decay constants in geo- and cosmochronology. Earth and Planetary Science Letters, 36, 359–362, doi: http://dx.doi.org/10.1016/0012-821X(77)90060-7.

[1]GSA Data Repository item 201Xxxx**,** geochronology and petrology methods and supplemental data, is available online at www.geosociety.org/pubs/ft20XX.htm, or on request from editing@geosociety.org or Documents Secretary, GSA, P.O. Box 9140, Boulder, CO 80301, USA.